ARRAYS OF MEMS-BASED ACTUATORS FOR CONTROL OF SUPERSONIC JET SCREECH

A.Naguib, C. Christophorou, E. Alnajjar and H. Nagib
Illinois Institute of Technology, Chicago, IL

C. C. Huang and K. Najafi
University of Michigan, Ann Arbor, MI

Abstract

The ability of a particular type of MEMS-based mechanical actuators to excite the shear-layer of a high-speed axisymmetric jet has been examined. This study focused on the utilization of a single actuator which is intended for use, as part of an array of actuators distributed around the jet lip, for the purpose of screech noise cancellation. Measurements of the streamwise velocity spectra on the shear layer centerline demonstrated the ability of the micron-size actuators to introduce disturbances into the shear layer up to a Mach number of 0.6. When the actuator oscillation frequency was close to the most unstable frequency of the shear layer, the disturbance magnitude exceeded that produced by acoustic and glow discharge forcing in other investigations. The ability of the MEMS actuator with its small amplitude and force to produce a strong disturbance was attributed to the direct mechanical action of the actuator on the shear layer at the high-receptivity point at the jet lip. It was demonstrated that an optimal radial actuator position exists where the actuator is within tens of microns from the jet lip. Finally, video records of the MEMS operation showed that the actuator operates properly and without being damaged under screech conditions.

Introduction

The ability to control separated shear layers has a great potential for impacting a wide range of engineering applications. For example, in flows over wings, turbine blades, etc., boundary layer separation occurs on the suction side at large angles of attack. Wygnanski and Seifert[1] have shown that "energization" of this separated shear flow using an oscillatory blowing technique resulted in separation control and localized increase in lift force.

In jet flows, a separated shear layer is encountered at the jet lip where the boundary layer on the wall of the jet nozzle emerges abruptly into the surrounding fluid. This highly unstable shear layer rolls up into large-scale vortical structures which are known to be, directly or indirectly, responsible for jet noise generation and mixing properties between the jet and surrounding fluid. By controlling the vortical structures developing in the shear layer, it is possible to achieve various types of control of the jet flow such as mixing enhancement and thrust vectoring; e.g., see Parekh et al[2].

Excitation of the shear layer in jet flows has been utilized in order to understand the flow dynamics and its noise generation and mixing characteristics as well as, more recently, to attempt to control the jet flow to arrive at various types of control objectives. The most common form of excitation has been via internal and external acoustic sources; e.g., Moore[3] and Corke and Kusek[4]. The popularity of acoustic forcing has been primarily due to ease of implementation and the ability to generate the high-frequency excitation required for forcing high-speed jet flows. However, the receptivity of the jet to acoustic excitation requires matching of the wavenumbers of the acoustic and instability waves (Tam[5]). Although such a condition is achievable in supersonic jets, at low Mach numbers the instability wave length is much smaller than the acoustic wave length. In this case, conversion of acoustic energy into instability waves is dependent on the "efficiency" of the unsteady Kutta condition at the nozzle lip.

Recently, Corke and Cavalieri[6] utilized a glow-discharge-based method to excite a jet flow at a Mach number of 0.85. The technique relies on heating the air between two electrodes positioned in the vicinity of the nozzle lip to the point where plasma occurs. This method has the advantage of being able to produce disturbances at frequencies up to 100 kHz, which makes it suitable for exciting high-speed jets. However, large driving voltages are required to produce the arching between the electrodes, and the energy expenditure required to drive the forcing is yet to be quantified.

In acoustic and glow-discharge forcing methods, conversion form acoustic and thermal energy, respectively, into kinetic (mechanical) energy of the flow instability must take place. A plausibly more efficient way of introducing disturbances into the shear layer is via direct mechanical action. Historically, studies utilizing mechanical actuators have been limited to low flow speeds due to the inability of the mechanical actuators to operate at the high-frequencies required to excite high-speed shear layers. Recently, Parekh et al[2] were able to utilize piezo-electric wedge actuators to excite low- and high-speed jet flows. The actuators, which were able to oscillate at a frequency of 5 kHz, were used to demonstrate the ability to control jets to produce enhanced mixing and thrust vectoring. Synthetic mm-size jets were also used by Smith and Glezer[7] to produce thrust vectoring in a rectangular high-aspect-ratio jet flow. In this case, two synthetic jets were positioned on the top and bottom and near the exit of the main jet. The jet controllability was demonstrated at a low jet velocity of 7 m/s.

The recent emergence of Micro-Electro-Mechanical-Systems (MEMS) has made possible the development of mechanical actuators that can operate at high frequency. Motivated by the problem of controlling supersonic screech, Alnajjar et al[8] investigated the ability of electrostatic-driven MEMS-based mechanical actuators to excite the shear layer of an axi-symmetric jet flow up to a Mach number of 0.42. The actuators, which had a characteristic size of tens of microns and an oscillation frequency and amplitude of 5 kHz and 23 μm respectively, were able to generate a flow instability at the forcing frequency. The magnitude of the generated disturbance amplified, through the linear instability mechanism of the shear layer, to a value similar to that associated with acoustic and glow discharge forcing. This occurred when the most amplified frequency of the shear layer was close to the oscillation frequency of the actuator. At the moderate Mach number value of 0.42, the small amplification rates associated with the relatively low value of the forcing frequency appeared to limit the magnitude of the generated disturbance to an order of magnitude below that of other types of forcing. These results were obtained utilizing only a single MEMS device, and hence the excited disturbances were localized, three dimensional, rather than axi-symmetric or helical.

The ability of the MEMS devices with their very small amplitudes to introduce disturbances in the jet flow at jet speeds up to that corresponding to a Mach number of 0.42 was attributed by Alnajjar et al[8] to the direct mechanical action of the actuators in the *immediate* vicinity of the high-receptivity point at the jet lip. The close positioning of the MEMS to the jet lip was made possible by the small size of the MEMS actuators. A few questions that arise however are: (1) is the reduction in the disturbance amplitude at the higher Mach number due to simply the reduction in amplification rate as suggested earlier, or is it due to improper functioning of the fairly fragile devices at the higher flow speeds? (2) Can the MEMS actuators provide strong enough forcing action to overcome the lower amplification rates at higher flow speeds? and (3) can the devices operate properly under the highly unsteady and harsh flow environment encountered during screech?

The current investigation addresses the above questions by utilizing the same type of MEMS actuators as those used by Alnajjar et al[8] but with a higher forcing frequency of 14 kHz. This allows forcing the jet at frequencies close to the most amplified frequency at larger Mach numbers. Additionally, well-controlled, strobed, and magnified video images of the MEMS actuators are used to carefully position the actuators in the vicinity of the jet lip (with microns accuracy) as well as to monitor the operation of the actuator while running the jet at speeds up to and including that corresponding to screech conditions. Finally, it should be noted that the current study was again conducted using only a single MEMS actuator.

Experimental Setup and Procedure

Flow Facility

All experiments reported here were conducted in the high-speed jet facility (HSJF) at IIT. The facility is a blow-down jet facility with a 1.0 inch diameter axisymmetric convergent nozzle exhausting into a ducted anechoic chamber. The jet stagnation pressure is maintained by a segmented ball control valve, pneumatic actuator and electro-pneumatic positioner. The compressed air supply system for the HSJF provides a maximum initial pressure of 210 psig contained in storage tanks that have a total volume of approximately 7,000 ft^3.

MEMS Actuators

The jet exit in the HSJF is fitted with a specially designed nozzle face to facilitate mounting and adjustment of an array of 16 MEMS devices positioned around the perimeter at the nozzle exit, as seen in Figure 1. Adjustment of the individual devices in the radial direction is achieved using micro-positioner traverses each with a total travel of 0.125 inches.

The MEMS chips used in this study were manufactured by the Center for Integrated Sensors and Circuits, Solid-State Electronics Laboratory at the University of Michigan. Figure 2 shows a SEM photograph of one of the electrostatic actuator devices used here. The device consists of a free-floating section which is mounted to the substrate underneath using elastic, folded beams. At the lower end of the floating section is a T-shaped actuator head with the approximate dimensions of 6 μm x 30 μm x 1300 μm. The actuator head is made to oscillate at an amplitude up to 70 μm and a resonant frequency of approximately 14 kHz using electrostatic comb drives (also seen in Figure 2). Also, notice the porous actuator structure which results in a reduced dynamic load on the actuator head. For more details on the construction and manufacturing of the actuators, see Huang et al[9].

During this study the actuator was driven using a combination of 20-Volt dc voltage and a 40-Volt peak-to-peak sinusoidal voltage. This resulted in a sinusoidal wave form varying between 0 and 40 Volts.

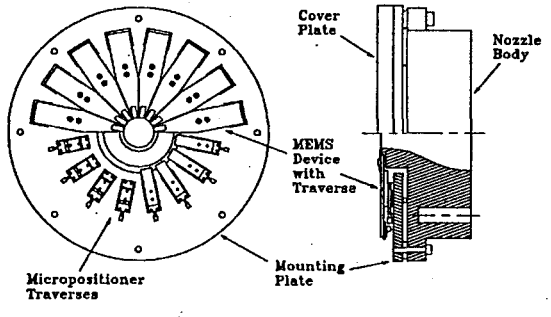

Figure 1. Mounting of MEMS Arrays on the Jet Facility

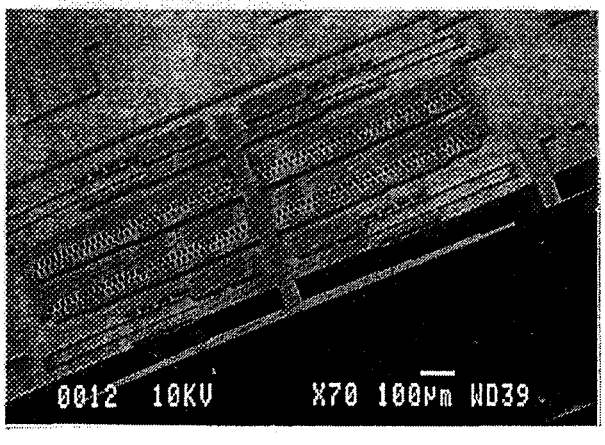

Figure 2. SEM View of the MEMS Actuator

Optical Observation System

After mounting of the MEMS device on the jet, its position was adjusted precisely with respect to the nozzle lip by direct observation of the MEMS actuator using a microscope with a magnification of about 50. When operating, the high frequency of oscillation of the MEMS device prohibited accurate determination of the location of the actuator at the two extreme ends of its motion. This problem was overcome by utilizing a fiber optic strobe light to illuminate the device during observation. A 60 Hz digitally-generated TTL pulse train was used to trigger the strobe. This resulted in a clearly observable "slow-motion" of the device and the location of the two extreme positions of the actuator with respect to the nozzle lip could be determined. This final step was achieved by using a CCD camera to display the video images on a Silicon Graphics Indy workstation, where measurements were done utilizing the screen pixels after appropriate calibration.

The same optical observation system described above was also used to visualize the operation of the MEMS actuator while running the jet up to speeds corresponding to screech conditions. However, in this case the microscope could not be positioned to view the MEMS from a location normal to the device since the microscope would then interfere with the jet flow. Instead, the microscope was positioned at an angle of about 45 degrees with respect to the jet center line, as shown in Figure 3. This oblique angle, combined with the relatively large working distance of the microscope allowed observation of the device during flow conditions without protrusion into the flow.

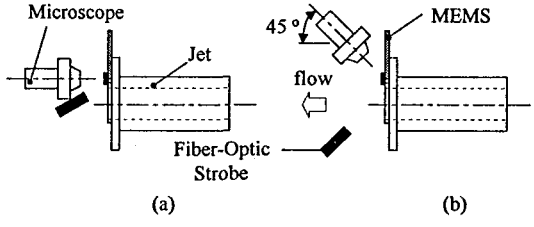

Figure 3. Optical Observation System: (a) MEMS Mounting, (b) MEMS Operation

Flow Conditions

The results presented here were obtained at jet speeds of 70, 140 and 210 m/s. The corresponding Mach (M_j) and Reynolds (Re_D: based on jet diameter) numbers are given in Table 1. The linearly most unstable frequency (f_o) of the jet shear layer for each of these velocities was estimated as $St_o\ U_j / \theta_o$; where, St_o is the most unstable Strouhal number set equal to 0.032 (e.g., see Ho and Huerre[10]), U_j is the jet speed

and θ_o is the initial momentum thickness of the jet shear layer.

Table 1. Jet Mach and Reynolds Numbers for Cases Investigated

U_j (m/s)	M_j	Re_D
70	0.2	118533
140	0.4	237067
210	0.6	355600

The initial momentum thickness was estimated by measuring the shear layer momentum thickness at various streamwise (x) locations close to the nozzle lip and extrapolating the results to x = 0. The resulting values of the initial momentum thickness are plotted versus the corresponding Reynolds numbers using open symbols in Figure 4. The data exhibits a power law behavior with an exponent of -0.49, as seen from the solid-line curve fit in the figure. This suggests that the boundary layer at the exit of the jet is laminar; since in this case, the dependence of θ_o on Reynolds number is expected to follow a power law behavior with a -0.5 exponent. The curve fit in Figure 4 was used to estimate the most unstable frequency for each of the speeds investigated here. The results are provided in Table 2.

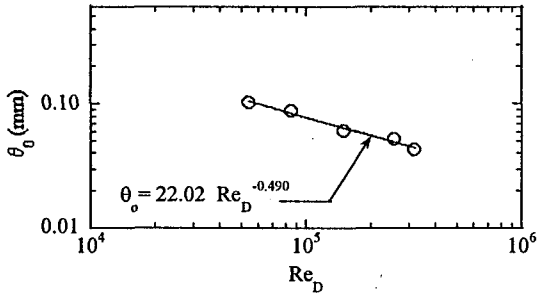

Figure 4. Initial Momentum Thickness of the Jet Shear Layer as a Function of Reynolds Number

Table 2. Initial Momentum Thickness and Most Unstable Frequency for Cases Investigated

U_j (m/s)	θ_o (mm)	f_o (kHz)
70	0.072	16
140	0.051	44
210	0.037	91

Comparison of the estimated most unstable frequency values with the oscillation frequency of the MEMS actuator used here (14 kHz) shows that the forcing frequency is approximately equal to one, one third and one sixth the most unstable frequency for the jet speeds corresponding to Mach numbers of 0.2, 0.4 and 0.6 respectively.

Data Acquisition and Analysis

All measurements were done using constant temperature hot-wire anemometry. A single-wire probe was used to measure time series of the streamwise velocity inside the shear layer. The full and mean-removed hot-wire signals were digitally acquired along with the MEMS actuator forcing signal. The mean-removed hot-wire signal was amplified to maximize the measurement resolution of the fluctuating signal. All three channels were digitized at the rate of 63000 samples per channel to provide a total of 102400 data points per timeseries.

To observe if the MEMS actuators introduce a disturbance into the flow, power spectra were estimated from the hot-wire measurements at the jet center line (where $U/U_j = 0.5$) using 512-point FFTs. Additionally, to estimate the energy of the disturbance caused by the MEMS actuators, a 512-point phase-averaged time record was generated from each time series. This was done by breaking the hot-wire timeseries into 512-point records which start at the same phase of the forcing cycle. These records were then averaged to produce the phase-averaged timeseries. Integration of the spectrum of this phase-averaged timeseries, after narrow-band-pass filtering around 14 kHz, provided the energy of the MEMS-forced disturbance at the forcing frequency.

Results and Discussion

Detection of MEMS Disturbance

The velocity spectra for the natural and forced jet flows at Mach number of 0.2 are shown in the top and bottom plots in Figure 5, respectively. The different lines in each of the plots represent spectra obtained at different streamwise locations. Except for two fairly small peaks at approximately 7 and 13 kHz, the spectra obtained in the natural jet seem to be wide-band, continuos and smooth.

When MEMS forcing is applied, a very strong peak is observed at the forcing frequency (Figure 7, bottom). The magnitude of the peak seems to rise initially with downstream distance and then fall. In addition to the peak at the forcing frequency, a second strong peak at 28 kHz is observed at all streamwise locations. A third peak is also depicted at a frequency of 21 kHz at the second and third x locations. The existence of multiple peaks in the spectrum at frequencies which are multiples of the forcing frequency and its subharmonic suggests that the MEMS-introduced disturbance has a large enough

amplitude to experience non-linear effects. These effects are responsible for the generation of instability modes at frequencies other than the forcing frequency. Overall, the spectrum appears to be dominated by the peaks resulting from the forcing.

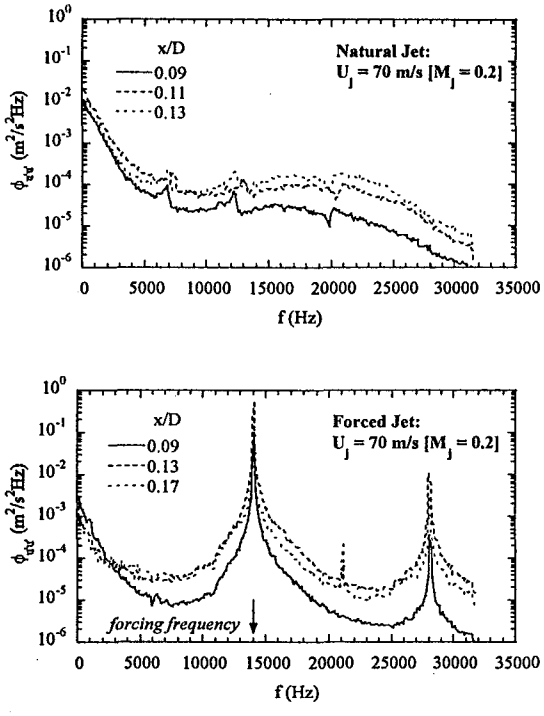

Figure 5. Streamwise Velocity Spectra for Natural (Top) and Forced (Bottom) Jet Conditions at $M_j = 0.2$

The disturbance spectra for the natural jet at M_j = 0.4 are shown in the top part of Figure 6. The corresponding spectra for the forced jet are shown in the bottom part of the figure. As seen from Figure 6, the natural jet spectra posses a fairly large and broad peak at a frequency of about 13 kHz. As seen from Table 2, the natural frequency of the jet at a Mach number of 0.4 is expected to be around 44 kHz. Therefore, the peak at 13 kHz does not seem to correspond to the natural mode of the shear layer or its subharmonic.

When operating the MEMS actuator, a clear peak is depicted in the spectrum at the forcing frequency. The peak magnitude initially magnifies to reach a magnitude of more than an order of magnitude larger than the fairly strong peak depicted in the natural spectrum at 13 kHz. The MEMS-induced peak is also significantly sharper than the "natural" peak. A second small peak, which is not seen in the natural spectrum, is also seen in the forced jet spectrum at the second harmonic of the forcing frequency (28 kHz) for the first two streamwise locations: x/D = 0.07 and 0.09.

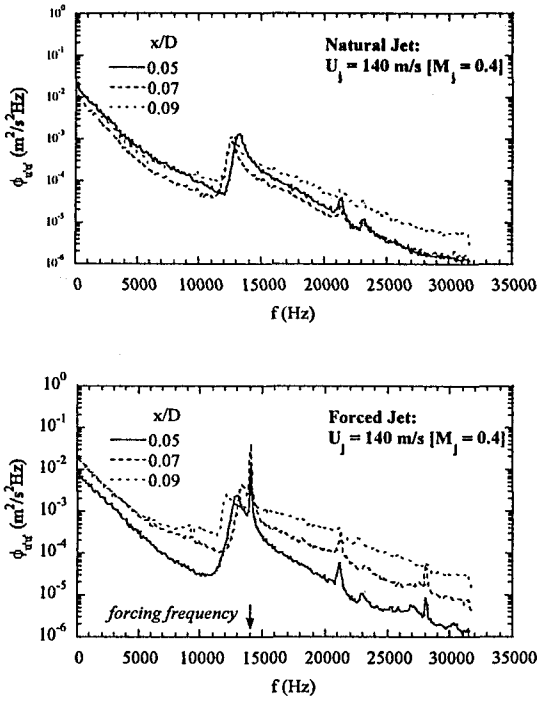

Figure 6. Streamwise Velocity Spectra for Natural (Top) and Forced (Bottom) Jet Conditions at $M_j = 0.4$

Finally, the spectra obtained at M_j = 0.6 are provided in Figure 7. Similar to the M_j = 0.4, a broad, fairly strong peak is depicted in the natural jet . The frequency of this peak appears to be about 16 kHz at x/D = 0.05 which is considerably lower than the estimated most unstable frequency of 91 kHz. The peak frequency value decreases with increasing x. This decrease in the peak frequency with x may be symptomatic of probe feedback effects (Hussein and Zaman[11]). Albeit this strong peak, when forced using the MEMS actuator, a clearly observable peak at the forcing frequency is depicted in the spectrum of the forced shear layer. Unlike, the results for the forced jet at Mach numbers of 0.2 and 0.4, the forced jet spectrum for M_j = 0.6 does not contain spectral peaks at higher harmonics of the forcing frequency.

Level of the MEMS-Induced Disturbance

To evaluate the level of the disturbance introduced into the shear layer by the MEMS actuator, the energy content of the spectral peak at the forcing frequency was calculated by making use of the phase-averaged spectra (see Data Acquisition and Analysis section for details). An example of a phase-averaged spectrum and how it compares to the conventional spectrum is shown in Figure 8 for a jet Mach number of 0.6.

As expected, the phase averaging process attenuates the energy across the entire frequency range except at the forcing frequency and related harmonics. The later, although undetectable for the case shown in Figure 8, have a significant contribution to the phase averaged spectrum at the lower Mach numbers. Therefore, all calculations of the disturbance energy at the forcing frequency were accomplished by integrating the phase-averaged spectrum after band-pass filtering to eliminate contributions from the other harmonics. The resulting disturbance *rms* value will be referred to as $<u_{rms,f}>$.

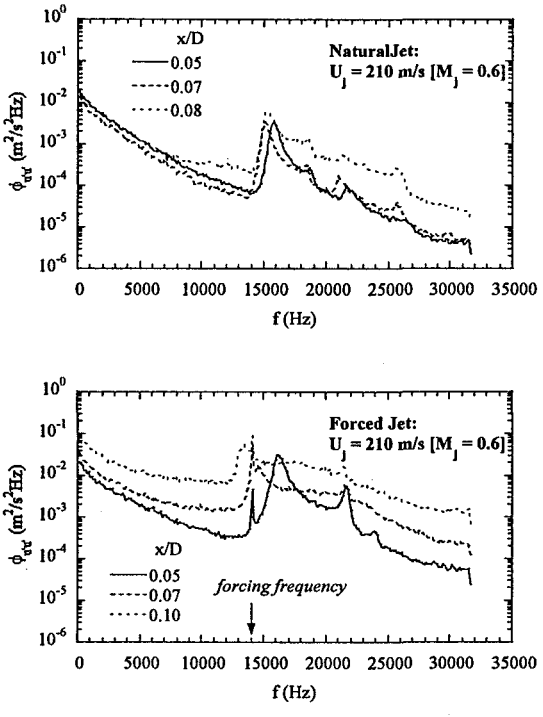

Figure 7. Streamwise Velocity Spectra for Natural (Top) and Forced (Bottom) Jet Conditions at $M_j = 0.6$

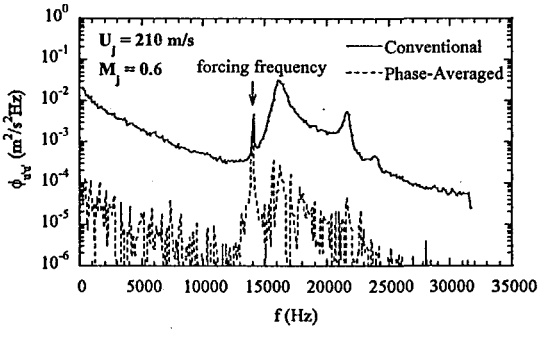

Figure 8. Conventional and Phase-Averaged Spectra for the Forced Jet At $M_j = 0.6$

The forced disturbance energy dependence on the streamwise location is shown for all three Mach numbers in Figure 9. The disturbance energy is normalized by the jet velocity and the streamwise coordinate is normalized by the jet diameter. Inspection of Figure 9 shows that for both $M_j = 0.2$ and 0.4 no region of linear growth is detectable. For these two Mach numbers, $<u_{rms,f}>$ only increases slightly before reaching a peak value followed by a gradual decrease in value: a process which is reminiscent of non-linear amplitude saturation.

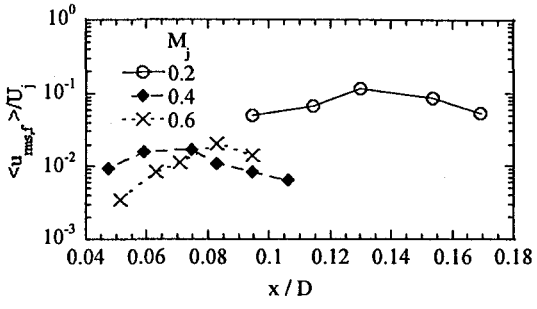

Figure 9. Streamwise Dependence of the Forced Disturbance Energy

Unlike the two lower Mach numbers, the disturbance energy for $M_j = 0.6$ appears to experience linear growth over the first four streamwise positions before saturating. It may be noticed also that only for $M_j = 0.6$, the disturbance rms level is appreciably lower than 1% of the jet velocity at the first streamwise location. In the work of Drubka et al[12], the fundamental and subharmonic modes in an acoustically-excited, incompressible, axi-symmetric jet were seen to saturate when their rms value exceeded 1-2% of the jet velocity. Therefore, it seems that the MEMS actuator is capable of providing an excitation to the shear layer that is sufficient not only to disturb the flow but also to produce non-linear forcing levels.

The magnitude of the MEMS forcing may also be appreciated further by comparison to other types of "macro-scale" forcing. To this end, the disturbance *rms* value produced by internal acoustic (Lepicovsky et al[13]) and glow discharge (Corke and Cavalieri[6]) forcing is compared to the corresponding rms values produced by MEMS forcing in Figure 10. The results for MEMS forcing contained in the figure are those from the current study using the high-frequency MEMS actuators as well as those from the earlier study by Alnajjar et al[8], using the same type of MEMS actuators but at a forcing frequency of 5 kHz.

As seen from Figure 10, for all cases of MEMS forcing, except that for the high frequency actuator/M_j = 0.2 and the low frequency actuator/M_j = 0.42, the MEMS-generated disturbance grows to a level which

is similar to that produced by glow discharge and acoustic forcing. For $M_j = 0.2$, the forcing frequency of 14 kHz is almost equal to the most unstable frequency of the shear layer (see Table 2) and the resulting flow disturbance is at a level which is significantly higher even than that produced by the "macro-scale" forcing methods.

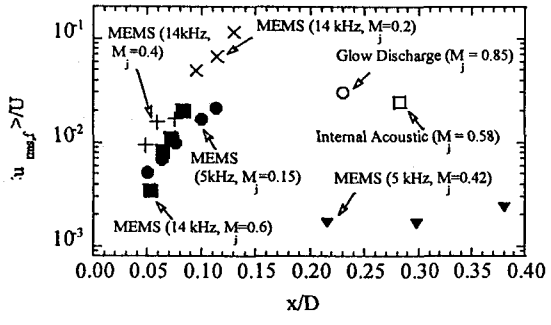

Figure 10. MEMS-Induced Disturbance Level Compared to Other Types of "Macro-Scale" Forcing

On the other hand, at $M_j = 0.42$, the 5 kHz MEMS actuator excites the flow at a frequency which is almost an order of magnitude lower than the most amplified frequency of the shear layer. The small amplification rate associated with a disturbance at a frequency which is significantly smaller than the natural frequency of the flow is believed to be responsible for the resulting small disturbance level at $M_j = 0.42$ when forcing with the 5 kHz actuator. However, as will be demonstrated in the next section, the level of the MEMS-generated disturbance is highly dependent on accurate positioning of the actuator at or very close to an optimal forcing location. For the results for $M_j = 0.42$, no special provisions were taken to ensure that the device was positioned as close as possible to its optimal position. This could affect the outcome by an order of magnitude (see next section).

Significance of the Jet Lip

The ability of the MEMS devices to excite flow disturbances at a level comparable to that produced by other large-scale forcing, notwithstanding the MEMS micron-size amplitude and force, is believed to be due to the ability to position the MEMS extremely close to the point of high-receptivity at the nozzle lip where the flow is sensitive to minute disturbances. To investigate this matter further, the radial position of the MEMS actuator with respect to the nozzle lip (y_{off}) was varied systematically. For all actuator positions, the flow was maintained at 70 m/s, while the actuator was traversed in the range from about 50 μm (outside the flow) to -150 μm (inside the flow) relative to the nozzle lip. The boundary layer at the exit of the jet at 70 m/s is believed to be laminar and has a momentum thickness of about 72 μm. Therefore, at its inner most location, the actuator is believed to penetrate into the flow a distance which is less than 20% of the boundary layer thickness, and hence, based on a Blasius profile, it is exposed to a velocity which is less than one fifth of the jet speed.

Figure 11 shows the streamwise velocity spectra obtained at x/D = 0.10, for the different radial positions of the actuator. Consideration of Figure 11 shows that a fairly strong dependence on the radial position of the actuator exists. In particular, the spectral peak at the forcing frequency increases by about two orders of magnitude as y_{off} changes from 37 μm outside the flow to -18 μm and -46 μm inside the flow, before the peak magnitude drops again. Also, at y_{off} = -18 μm and -46 μm, large disturbance amplitude levels appear to result in strong non-linear effects, as depicted by the existence of fairly strong peaks at harmonics of the forcing frequency.

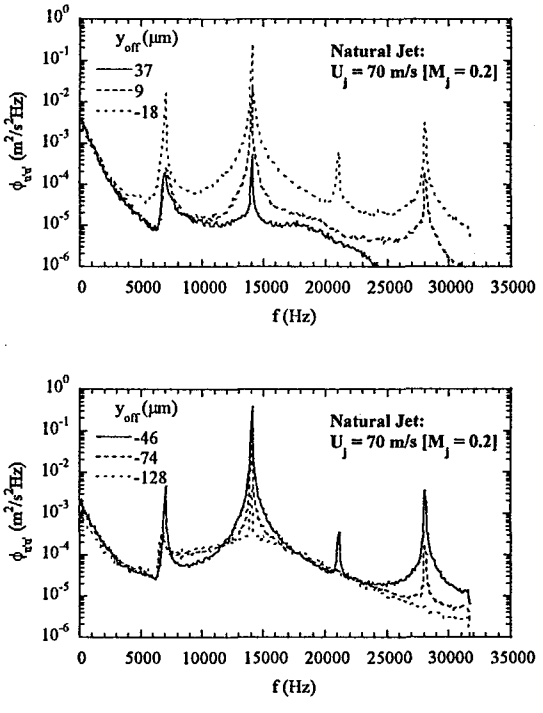

Figure 11. Effect of MEMS Actuator Radial Position on the Streamwise Velocity Spectrum

The energy content of the spectral peak at the forcing frequency was calculated for all the spectra shown in Figure 11. The results are displayed in Figure 12 as a function of the actuator radial position. For reference, a dimension indicating the momentum thickness of the boundary layer emerging at the exit of the jet is included in Figure 12.

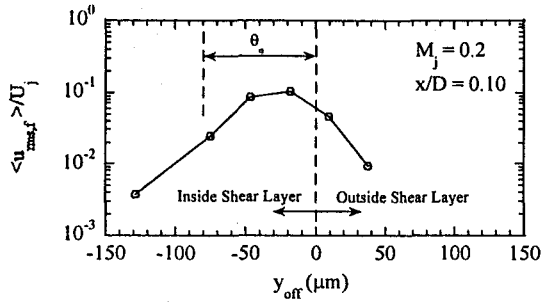

Figure 12. Effect of MEMS Actuator Radial Position on the Generated Shear Layer Disturbance Level

As seen from the figure, the largest disturbance energy is produced when the actuator is closest to the nozzle lip ($y_{off} = 0$) and into the flow. If the actuator is placed a distance as small as 75 μm off the position corresponding to the maximum shear layer response, an order of magnitude reduction in disturbance rms value is observed. Figure 12 highlights the significance of the ability to force the shear layer in the immediate vicinity of the jet lip, as discussed earlier.

Observation of MEMS Operation

The MEMS actuator operation was observed during various flow conditions using the optical observation system described in the Experimental Setup and Procedure section. During the observation process the MEMS actuator position was maintained flush with the jet lip. The flow speed was increased incrementally from no flow up to screech conditions. A video tape was obtained of the actuator operation. Inspection of the video tape revealed that the MEMS actuator operated properly over the entire flow range with no damage or stoppage due to the large flow speeds and highly unsteady conditions associated with screech.

Conclusions

It has been demonstrated that a certain design of MEMS-based mechanical actuators is able to operate properly under screech conditions as well as to introduce disturbances into the shear layer of an axisymmetric jet up to a Mach number of 0.6. The level of the introduced disturbance was generally high and reached non-linear saturation levels for a range of operating conditions. When the actuator frequency was close to the natural frequency of the jet, the excited disturbance level was higher than that encountered using acoustic and glow discharge forcing in other investigations. It was also demonstrated that the disturbance level was strongly dependent on the proximity of the actuator to the jet lip, or the high receptivity point in the flow. The ability of the MEMS device with its small size to operate in close proximity to the jet lip is believed to be responsible for its ability to excite strong flow disturbances, albeit the small amplitude and force of the actuator. The performance of the actuator at higher Mach numbers is to be investigated next.

Acknowledgments

The authors greatly appreciate the support of the Air Force Office of Scientific Research (AFOSR-F49620-93-1-0459, AFOSR-F49620-94-0184 and AFOSR-F49620-96-1-045) monitored by Drs. Jim McMichael and Mark Glauser.

References

1.Wygnanski, I. and Seifert, A. 1994. "The Control of Separation by Periodic Oscillations". *AIAA* Paper 94-2608.

2.Parekh, D. E., Kibens, V., Glezer, A., Wiltse, J. M. and Smith, D. M. 1996. "Innovative Jet Flow Control: Mixing Enhancement Experiments". *AIAA* Paper 96-0308.

3.Moore, C. J. 1977. "The Role of Shear-Layer Instability Waves in Jet Exhaust Noise". *J. Fluid Mech.* **80**, part 2, pp. 321-367.

4.Corke, T. C. and Kusek, S. M. 1993. "Resonance in Axisymmetric Jets with Controlled Helical-Mode Input". *J. Fluid Mech.* **249**, pp. 307-336.

5.Tam, C. K. W. 1986. "Excitation of Instability Waves by Sound- A Physical Interpretation". *Journal of Sound and Vibration* **105** (1), pp. 169-172.

6.Corke, T. C. and Cavalieri, D. 1996. "Mode Excitation in a Jet at Mach 0.85". *49th American Physical Society Meeting, DFD,* Syracuse, NY.

7.Smith, B. L. and Glezer, A. 1997. "Vectoring and Small-Scale Motions Effected in Free Shear Flows Using Synthetic Jet Actuators". *AIAA* Paper 97-0213.

8.Alnajjar, E., Naguib, A. M., Nagib, H. M. and Christophorou, C. 1997. "Receptivity of High-Speed Jets to Excitation Using An Array of MEMS-Based Mechanical Actuators. Proceedings, 1997 *ASME Fluids Engineering Division Summer Meeting.* Paper FEDSM97-3224.

9.Huang C. C., Papp, J., Najafi, K. and Nagib, H. M. 1996. "A Microactuator System for the Study and Control of Screech in High-Speed Jets". Proceedings, *1996 Micro Electromechanical Systems Workshop (MEMS 96)*, San Diego, California.

10.Ho, C. M. and Huerre, P. 1984. "Perturbed Free Shear layers". *Ann. Rev. Fluid Mech.* **16**, pp. 365-424.

11.Hussain, A. K. M. F. and Zaman, K. B. M. Q. 1978. "The Free Shear Layer Tone Phenomenon and Probe Interference". *J. Fluid Mech.* **87b**, 2, pp. 349-384.

12.Drubka, R. E., Reisenthel, P. and Nagib, H. M. 1989. "The Dynamics of Low Initial Disturbance Turbulent Jets". *Phys. Fluids A* **1**(10), pp. 1723-1735.

13.Lepicovsky, J., Ahuja, K. K., and Burrin, R. H. 1985. "Tone Excited Jets, Part III: Flow Measurements". *Journal of Sounda and Vibration* **102** (1), pp. 71-91.